On the reliability of an optical fibre probe in bubble column under industrial relevant operating conditions

H. Chaumat [a], A.M. Billet-Duquenne [a,*], F. Augier [b], C. Mathieu [b], H. Delmas [a]

[a] *Laboratoire de Génie Chimique, CNRS UMR 55-03, B.P. 1301, 31106 Toulouse Cedex 1, France*
[b] *Rhodia, Centre de Recherche de Saint Fons, France*

Abstract

When bubble columns are operated under industrial relevant conditions (high gas and liquid flow rates, large bubbles and vortices,...), local data, and especially bubble size values, are difficult to obtain. However, such data are essential for the comprehension of two-phase flow phenomena in order to design or to improve industrial installations.

When high gas flow rates and organic liquids are used, intrusive optic probes are considered. This work investigates different ways to derive reliable local information on gas phase from double optic probe raw data. As far as possible, these results have been compared with global data, easier to measure in such conditions.

Local gas hold-up, ε_G, and bubble frequency, f_B, are easily obtained, but bubble velocity and bubble diameter determination is not obvious. For a better reliability, the final treatment that is proposed for velocity and size estimation is based on mean values only: the bubble velocity is considered as the most probable velocity $\tilde{v}$ issued from raw signals inter-correlation function and the mean Sauter diameter is calculated through $d_{SM} = \frac{3\tilde{v}\varepsilon_G}{2f_B}$.

Keywords: Bubble column; Gas–liquid flow; Measurement technique; Optic probe; Signal treatment

1. Introduction

Local characteristics of flow and phase distribution are crucial to model and enhance mass transfer flux in multiphase reactors, but difficult to acquire.

Flows in bubble reactors may be complex and chaotic, all the more when these reactors are used under relevant industrial operating conditions. They usually show heterogeneous bubbling regime: the high gas flow rate generates bubble swarms and large intense liquid vortices, leading to high level of turbulence and highly distorted bubbles.

In these severe conditions, it is therefore difficult to perform reliable experimental investigations. Non-invasive techniques, like camera imaging or tomography techniques [1], cannot be applied, due to large pilot dimensions, high gas hold-up and highly fluctuating flow. Wall pressure transducers seem to be appropriate to most gas–liquid processes; however they usually provide space averaged values only (mean gas hold-up between the axial positions of two transducers).

Use of invasive techniques is also critical: due to pressure or corrosive fluids, it may be difficult to settle probes through pilot wall. What is more, most of the invasive techniques require specific precautions that may not be consistent with reactor operating conditions. For instance, hot film anemometry can be used in two-phase flows for investigation of gas hold-up and liquid velocity [2,3], but a strict temperature uniformity is necessary to derive reliable velocities. Classical Pitot tubes have to be flow oriented [4], which is quite impossible to achieve in recirculating flows.

To get various local characteristics of gas phase, optical fibre probes are often chosen [5]. These probes can be very

* Corresponding author. Tel.: +33 534615256; fax: +33 534615253.
E-mail address: AnneMarie.Billet@ensiacet.fr (A.M. Billet-Duquenne).

Nomenclature

d_{SM}	Sauter mean diameter (m)
f_B	bubble frequency (bubble/s)
k	inter-correlation coefficient
l_{12}	inter-tip distance (m)
N	associated bubble number
N_{12}/N_1	proportion of associated bubbles compared to bubbles detected by the front fibre
r	radial position in the column (m)
R	column radius (m)
$R(\tau)$	inter-correlation function of two fibres binarized signals
u_G	superficial gas velocity (m/s)
v_G	gas phase velocity (m/s)
v_i	velocity of i bubble (m/s)
$\bar{v}$	bubble arithmetic mean velocity (m/s)
$\tilde{v}$	most probable bubble velocity (m/s)
X_i	binarized signal of i fibre

Greek letters

α	parameter for minimum acceptable flying time
β	parameter for maximum acceptable flying time
Δt_i	flying time of i bubble (s)
ε_G	gas hold-up
σ	velocity distribution width (m/s)
τ_{max}	most probable flying time (s)

thin but also quite robust if needed. This technique directly provides local gas hold-up and bubbling frequency even if the sensor is not strictly flow oriented. With a specific signal treatment and under some assumptions, it may also derive bubble velocity and bubble size [6–8]. But the assumptions to be made are restrictive: exclusively vertical bubble motion, isotropy of turbulence and regular bubble shape (spherical or ellipsoidal).

This kind of treatment has been tested by the authors for chains of distorted tumbling bubbles [9]. In this case, bubble velocity distributions can be obtained, provided that some adjustable parameters, linked to the range of expected bubble velocities, are well defined. However, bubble size distribution turns out to be very difficult to obtain, due to distorted shapes and chaotic motion of bubbles: these conditions are far from the classical hypothesis used for data treatment. Nevertheless, the mean bubble velocity and the mean Sauter diameter have been found more meaningful, because their derivation requires data of gas hold-up, bubble frequency and most probable velocity (issued from inter-correlation of both signals) only.

The objective is now to test this treatment in a more complex flow (high bubble density, liquid and bubble loops). The present work deals with the reliability of measurements performed with a double optic probe in highly aerated bubble flow. Experiments are performed in a pilot bubble column, filled with water or with cyclohexane, and operated under high gas flow rate: these conditions are similar to industrial ones. Local data acquired by means of a double optic fibre probe are presented and analyzed. Gas hold-up, bubble velocity and mean Sauter diameter are derived and their reliability is discussed.

2. Optic probe technique

2.1. Principle

Gas phase characterization using double optic probes is a well-known technique: an infrared light is generated from an opto-electronic box and is injected into each glass fibre. Due to the difference in refractive index between gas and liquid, this light is reflected when the fibre tip lays in gas and refracted when it lays in liquid (Snell law). After signal amplification, this system delivers crenels type voltage outputs (Fig. 1), in which high and low parts correspond to gas and liquid phase respectively.

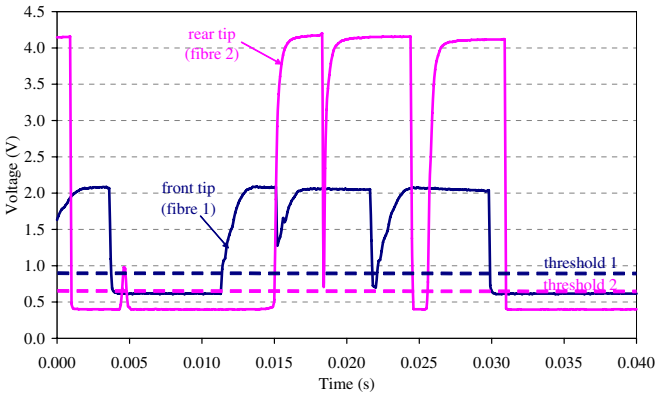

Fig. 1. Example of raw signals.

2.2. Treatment

To clearly distinguish gas and liquid, the crenel signals are binarized by use of an appropriate threshold. As the rise and fall times are finite, a particular attention should be paid to the threshold choice. Two methods are classically used:

- Some authors use the threshold value that minimizes the difference between the mean gas hold-up, issued from the integration on a section of the local gas hold-up, and the mean gas hold-up measured in another way [10,11].
- For most authors, the threshold is expressed as a fraction of the crenel height; this fraction varies between 5% and 80% depending on authors [2,12–14].

In our case, a preliminary study shows that the gas hold-up varies by about 5% depending on the threshold choice (between 2% and 20% of crenel height); this dependence is negligible in comparison with other further uncertainties. The threshold is then chosen at around 10% of the crenels height to eliminate the noise, as done by Utiger et al. [2].

For a given fibre (the front one in general, "fibre 1"), the gas hold-up, ε_G, corresponds to the ratio between the cumulative times that the fibre tip has in gas and the total acquisition time; the bubble frequency, f_B, corresponds to the number of bubbles detected by time unit.

The probability density function of bubble velocities may be established, assuming no deformation, no deviation nor rotation of bubbles during their flight from tip to tip. In this way, the crenels from the two fibres that correspond to the same bubble have to be correctly associated. Let us call τ_{max} the maximum of the inter-correlation function of the two signals, corresponding to the most probable flying time between both fibres:

$$\tau_{max} = \max(R(\tau)) \tag{1}$$

$$\text{with } R(\tau) = \int_0^\infty X_1(t)X_2(t+\tau)\mathrm{d}t \tag{2}$$

where X_i is the binarized signal of fibre i.

It is then checked for a crenel detected at t time on front tip signal, whether a crenel lays on rear tip signal within a given delay bounded by $\alpha\tau_{max}$ and $\beta\tau_{max}$ [15], where α $(0 \leqslant \alpha \leqslant 1)$ and β $(\beta > 1)$ are parameters linked to the velocity range (Fig. 2). As shown in a precedent study [9], a pertinent choice of α and β values is essential to derive a reliable distribution; however satisfying values for α and β are difficult to select a priori.

The mean velocity, $\bar{v}$, is the arithmetic mean of individual bubbles velocities (issued from the crenel association):

$$\bar{v} = \frac{1}{N}\sum_{i=1}^{N} v_i = \frac{1}{N}\sum_{i=1}^{N} \frac{l_{12}}{\Delta t_i} \tag{3}$$

A mean value of bubble velocity can also be estimated from the most probable velocity, $\tilde{v}$, that is derived using the most probable flying time, τ_{max} (corresponding to the two signals inter-correlation maximum), and the inter-tip distance, l_{12} [12,16]:

$$\tilde{v} = \frac{l_{12}}{\tau_{max}} \tag{4}$$

The mean Sauter diameter is deduced from [17]:

$$d_{SM} = \frac{3\tilde{v}\varepsilon_G}{2f_B} \tag{5}$$

3. Experimental setup

3.1. Pilot plant

Optic probe measurements are performed in a stainless steel bubble column of 1.6 m in height and 0.2 m in diameter (Fig. 3). The column is filled with water or cyclohexane. The gas is sparged through two concentric perforated torus (diameter: 0.11 and 0.16 m, orifice size: 0.001 m). When cyclohexane is used, the gas outlet is collected at the top of the column; it is then taken to a specific cryogenic apparatus (CIRRUS, Linde Gas) so that it can be cleaned from any trace of organic vapor before reaching atmosphere.

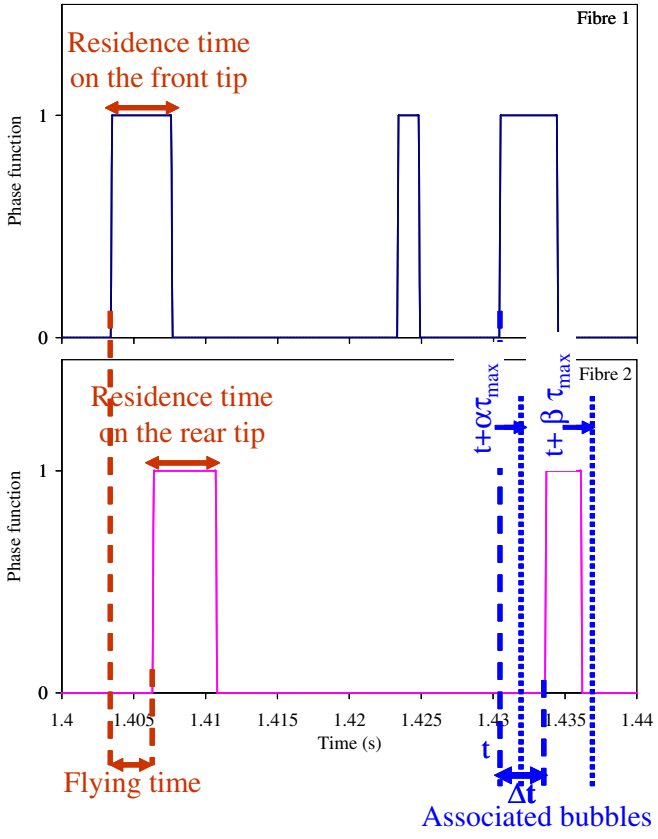

Fig. 2. Interval of search on raw signal 2 for crenels association.

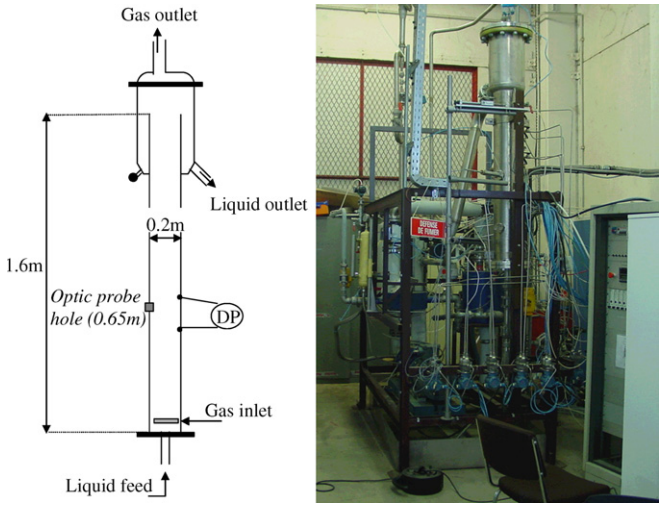

Fig. 3. Pilot bubble column.

Gas superficial velocity u_G ranges up to 0.12 m/s for cyclohexane case and up to 0.30 m/s for water case. The whole setup is run at 20 °C and atmospheric pressure.

Note that the experiments presented here are run in batch conditions in regard with liquid phase, as it has been observed that the superficial liquid velocity does not have a significant influence on probe treatment validity until 0.1 m/s (maximum superficial liquid velocity value tested).

The optic probe is settled through the column wall, at the axial position of $z = 0.65$ m. Once settled, it can be moved along the column diameter, to investigate radial profiles of gas phase characteristics. The column wall is also equipped with a differential pressure transducer (DP). It measures the apparent density of fluid (gas–liquid mixture) around optic probe position. From this value of apparent density, the average gas hold-up (ε_G) in this column part can be deduced, as well as gas phase average velocity, v_G ($v_G = u_G/\varepsilon_G$).

3.2. Optic probe

The probes used for this study are commercial double optic sensors (RBI). Each double probe is made of two 40 μm glass fibres whose tips are re-enforced by two sharp sapphire pins (Fig. 4). The double probe is mounted inside a thin stainless steel bended support, so that it always faces the mean flow. A small distance between probe tips (l_{12}) is chosen (0.001 m in this work).

The signal is acquired through a data card (National Instruments) and a computer.

The crossing bubbles have to be precisely described. For this purpose, an acquisition frequency of 10 kHz is recommended to perform an accurate crenels description. This frequency is also sufficient to cover the whole velocity range, as it allows axial velocity measurements up to 10 m/s (frequency × inter-tip distance).

The record duration must be longer than the longest characteristic time scale of hydrodynamic phenomena (large liquid loops, oscillating gas plumes,...) and, on the second hand, it has to allow a sufficiently large number of bubbles to obtain relevant bubble velocity and bubble size data. 1000–2000 'associable' bubbles are needed to collect reliable results [3,10,18–20].

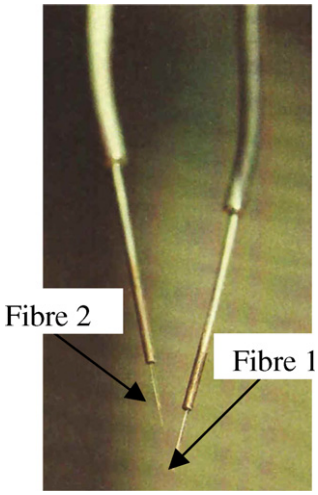

Fig. 4. RBI double optic probe.

- The first criterion is verified if, for given experimental conditions, measured data (gas hold-up for example) does not depend on recording time. In this study, tests have shown that the minimum recording time increases with gas flow rate and varies with radial location of the measuring point. For the highest gas superficial velocity used here, a recording delay of 100 s gives reproducible results on column axis, whereas 130 s are needed near the column wall.
- Concerning the second criterion, based on statistical arguments, the previous times are not long enough; a record duration of 200 s is needed, except near the column wall, where low gas hold-up and average downward liquid flow allow few bubbles to touch both fibres. In this part of the column, 400 s are found sufficient to detect 2000 'associable' bubbles per record.

The data treatment is derived using Matlab software.

4. Optic probe application in bubble column

To test the signal treatment process, the raw signal is first examined. Then, the reliability of gas hold-up measurements is verified. At last, the complex problems of velocity and diameter determinations are checked.

The results that were chosen to be presented in this part concern mainly experiments run in cyclohexane as liquid phase, as results in organic media are rarely reported in the literature.

4.1. Raw signal

An example of a raw signal is presented in Fig. 1. For both probes it can be observed that:

- The ratio 'signal to noise' is high.
- Between two bubbles, each signal lays under the threshold level (dotted lines in Fig. 1), making sure that two bubbles cannot be wrongly considered as a unique large one.
- As expected, the signal rise, corresponding to glass fibre drying, takes a longer time than the downward fall, corresponding to fibre wetting. However, it has been proved that the threshold choice has no significant influence on the gas hold-up nor on the most probable velocity.

If the two signals are compared, it appears that, in cyclohexane, the number of bubbles detected through front fibre is greater than the number of bubbles pierced by the rear fibre: on their way towards the rear tip, bubbles may be deviated by the front tip. As a consequence and as fre-

quently observed [8,13,21], lower gas hold-up values could be derived from the rear probe. In the following, the gas hold-up data are then issued from the front tip.

4.2. Gas hold-up

Fig. 5 presents radial profiles in gas hold-up issued from water and cyclohexane experiments. They show a classical bell shape, with higher values at column axis than in wall region. It is also verified that the gas hold-up increases with gas superficial velocity.

In heterogeneous bubble columns, time averaged downward liquid velocity is usually found in the vicinity of wall, around $r/R = 0.7$ [22–24]. Therefore small bubbles following the liquid downflow could miss the fibre tips; the gas hold-up is then under-estimated. To check the reliability of local gas hold-up data in these conditions, a validation test is needed.

In this purpose, the mean gas hold-up, resulting from the integration of gas hold-up values over a column section (assuming $\varepsilon_G = 0$ at the wall, $r = 0.1$ m), is compared to the mean gas hold-up deduced from differential pressure transducers measurements (DP, see Fig. 3). In cyclohexane, mean hold-up and integrated local values fit well (Fig. 6): the maximum relative error observed is 10% for $\varepsilon_G < 20\%$ (corresponding to $u_G < 0.08$ m/s). At higher gas velocity, as expected, some under-estimation of the overall gas hold-up with optic probe is observed, especially in water. Nevertheless the agreement between both methods is suitable until $\varepsilon_G = 25\%$ ($u_G = 0.15$ m/s, less than 20% difference). In the core area, when the flow is ascendant in average, the gas hold-up issued from optic probe will also be considered significant in the whole gas velocity range.

As a conclusion, the gas hold-up estimated in this work by optic probe is reliable till $u_G = 0.15$ m/s, but for $u_G > 0.15$ m/s it is under-estimated in the vicinity of wall, where the wall does not face to the probe.

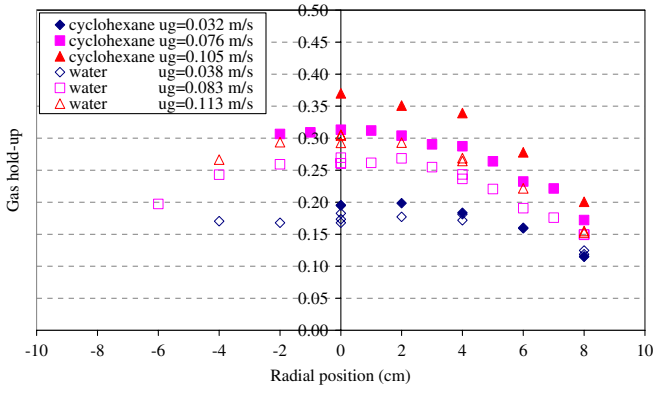

Fig. 5. Radial profiles in gas hold-up.

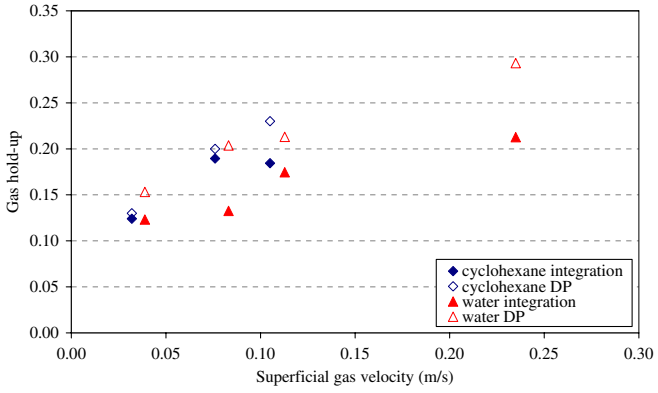

Fig. 6. Validation of local gas hold-up measurements.

4.3. Bubble velocity

Measurement of individual bubble velocity is critical, as the use of both fibre data is needed, as well as the bubble association, which may lead to some uncertainty.

In this part, two procedures are tested:

- The mean velocity can be estimated through the arithmetic mean of individual bubble velocities, $\bar{v}$. This approach generates a lot of information, but it needs an accurate crenel association method.
- The mean velocity can be considered as the most probable velocity, $\tilde{v}$, directly issued from the inter-correlation maximum of both signals.

4.3.1. Bubble velocity distributions

In order to determine the velocity distribution at a measurement point, the association of the crenels corresponding to the same bubble is a crucial step. As in the former study [9], the flows studied here should lead to association difficulties resulting from chaotic bubble paths. Additional difficulties can also be encountered, due to high bubble density and downward flowing bubbles: crenels induced by two distinct bubbles are likely to be associated.

To limit wrong associations, a short inter-tip distance is better ($l_{12} = 0.001$ m). The association is then realised through parameters α and β, as described in paragraph 2.2. Classically, α and β, which characterize the bubble velocity range, are chosen equal respectively to 0.5 and 1.5 [3]. See as an example Fig. 7, showing the arithmetic mean bubble velocity profiles obtained in cyclohexane ($\alpha = 0.5$, $\beta = 1.5$).

Larue de Tournemine [3] reports results collected in a squared section bubble column for a very low gas flow rate, corresponding to homogeneous gas dispersion. In this case, the derived velocity distribution is not very sensitive to values of α and β: when using the interval $(\alpha;\beta) = (0;2)$, instead of $(0.5;1.5)$, the mean derived velocity $\bar{v}$ differs by 4% only and distribution width σ increases by 31%. In our pilot, a similar test, realised in highly heterogeneous bubble flow with cyclohexane and water, leads to variations up to 62% on $\bar{v}$ and up to 620% on the distribution width σ (Table 1). Parameters α and β have a strong

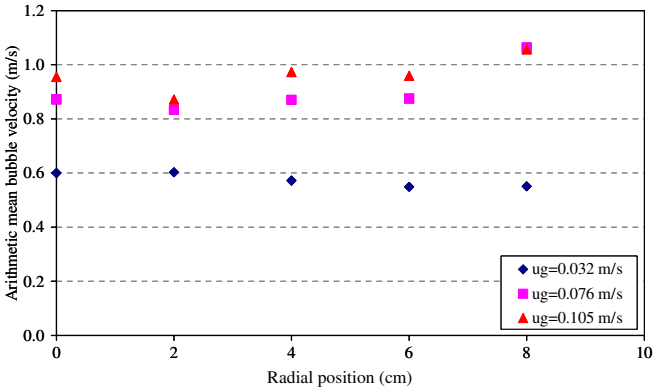

Fig. 7. Arithmetic mean velocity profiles (cyclohexane) ($\alpha = 0.5; \beta = 1.5$).

Table 1
Effect of α and β values on the mean velocity and on the distribution width

Medium	u_G (m/s)	$\bar{v}$ (m/s)		σ (m/s)	
		(0;2)	(0.5;1.5)	(0;2)	(0.5;1.5)
Water	0.235	1.34	2.55	0.39	3.28
Cyclohexane	0.105	0.96	1.46	0.30	1.87

influence on the derived velocity distributions at high gas fraction.

Fig. 8a and b presents the influence of α and β values: the flying time distribution is derived for a given raw signal (respectively in cyclohexane and water) and for various (α, β) sets. The results exhibit discrepancies. Contrary to data obtained in a little tank [9], the observed number of bubbles showing the same flying time depends on α and β, especially in water at high gas velocity: though l_{12} is weak, some crenels are associated in different ways, depending on α and β, mainly because of high bubble concentration.

To limit the wrong crenels associations, a criterion on residence time may be added: Kalkach-Navarro et al. [25] and Lo and Hwang [14] suggested that, to be associated, the crenels should have similar residence time on both fibres, increasing the probability that the two crenels are induced by the same bubble and that the bubble motion is vertical. This method is particularly interesting when the inter-tip distance is of the order of magnitude of bubble diameter; it is a priori less attractive in this work, as the small inter-tip distance favors similar residence times, but it is tested though.

We arbitrary choose to associate bubbles whose residence time differs of less than 20%. Under this criterion on residence time, the effect of α and β is re-evaluated (Fig. 9); the problem of wrong crenels association nearly vanishes; the crenels look properly associated. However, flying times lesser than 2×10^{-4} m/s are observed when $\alpha = 0$. As a consequence, the associated velocity distributions, presented in Fig. 10 for cyclohexane, exhibit that more than 5% of the bubbles are faster than 5 m/s.

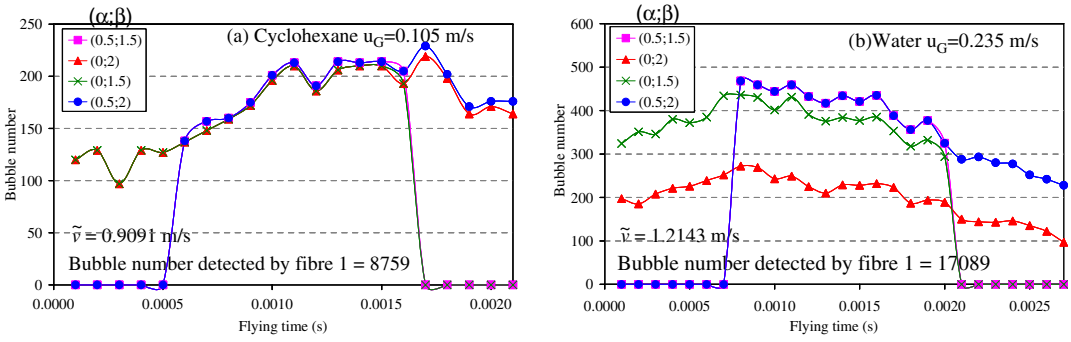

Fig. 8. Effect of α and β values on flying time distribution (PDF) without residence time condition.

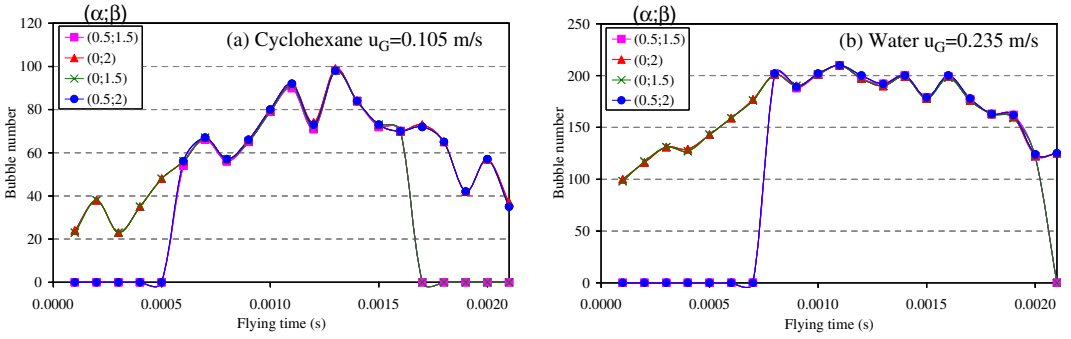

Fig. 9. Effect of α and β values on flying time distribution (PDF) with residence time condition.

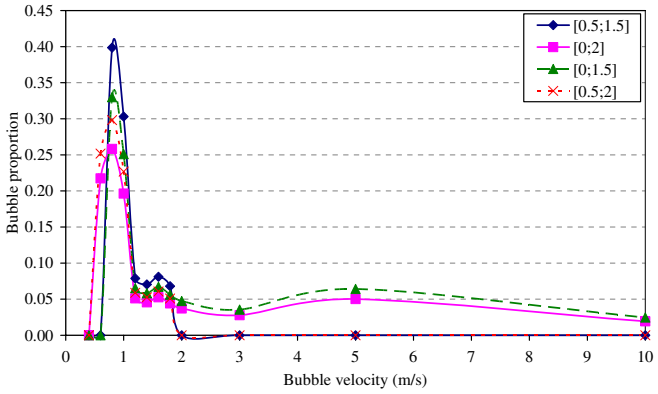

Fig. 10. Associated bubble velocity distribution (cyclohexane, $u_G = 0.105$ m/s).

Even if the crenels are correctly associated, the deduced velocity can show erroneous values. Due to short inter-tip distance, a bubble having a non-negligible radial velocity can touch both fibres nearly at the same time and lead to similar residence time on both fibres (Fig. 11). Note that the additional condition on residence time suppresses about 40% of the smallest residence time events (observed for $\alpha = 0$, when short flying time are allowed). However, this filter is not sufficient to completely eliminate radial velocities effect.

Table 2 compares the results with those obtained without any residence time criterion, and for different α and β values. This table presents $\bar{v}$ data and the bubble number proportion (N_{12}/N_1), defined as the ratio between the number of associated bubbles and the total number of bubbles detected by the first fibre.

Obviously, this additional criterion reduces the bubble number proportion (N_{12}/N_1). The proportion of treated bubbles diminishes by more than 75%, especially in the wall vicinity. This additional condition acts as a selective filter.

As a consequence of radial motion of bubbles, the mean velocity still strongly depends on α and β (Table 2): as α and β values cannot be chosen a priori, no exact mean velocity nor velocity distribution can be deduced from this method with chaotic flows.

4.3.2. Most probable bubble velocity

The alternative method for velocity estimation is based on the most probable velocity $\tilde{v}$. The most probable velocity is very interesting, as it is based on the inter-correlation function maximum, which acts as a mathematic filter: the associated bubbles having non-vertical trajectory are excluded, as they are in statistical minority (see bubble proportion having high bubble velocity, for $\alpha = 0$, in Fig. 10). $\tilde{v}$ has then a physical meaning and does not depend on treatment parameters.

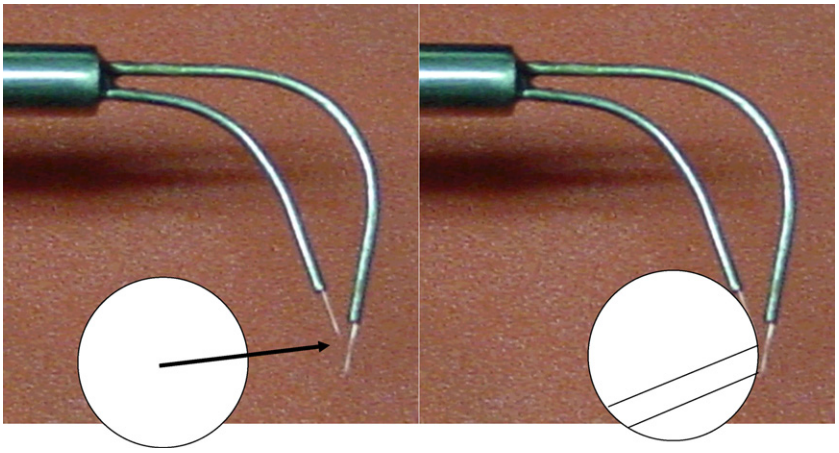

Fig. 11. How a bubble can touch both fibres simultaneously and give similar residence time on both fibres.

Table 2
Effect of the residence time criterion on the mean velocity and on the association bubble number proportion ($r = 0$ m)

Medium	u_G (m/s)	$(\alpha;\beta)$	$\tilde{v}$ (m/s)	$\bar{v}$ (m/s)		N_{12}/N_1 (%)	
				No constraint	Constraint	No constraint	Constraint
Water	0.235	(0.5;1.5)	1.21	1.34	1.34	32	14
		(0;2)		2.55	2.24	53	24
		(0;1.5)		2.95	2.56	44	20
		(0.5;2)		1.18	1.20	43	18
Cyclohexane	0.105	(0.5;1.5)	0.90	0.96	0.96	24	9
		(0;2)		1.46	1.29	40	15
		(0;1.5)		1.78	1.50	30	11
		(0.5;2)		0.82	0.85	35	13

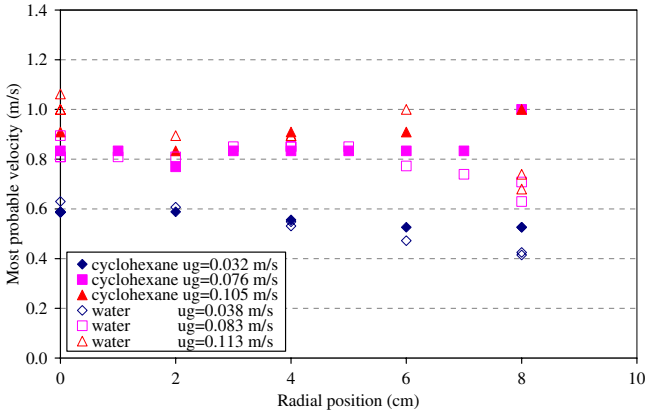

Fig. 12. Most probable velocity profiles.

Examples of most probable bubble velocity profiles are presented in Fig. 12 for both liquid media. The velocity values, ranging between 0.4 and 1 m/s, are consistent with literature, as these values lay between the terminal velocity and the bubble velocity observed in gaslift (see [14] for example). Note that this velocity is similar to the mean velocity $\bar{v}$ obtained with $\alpha = 0.5$ and $\beta = 1.5$. The most probable bubble velocity increases with superficial gas velocity, but is very similar for the two liquids. As expected, bubble velocity slightly decreases near the wall, except for cyclohexane at high superficial gas velocity. This decrease is more pronounced in water than in cyclohexane. Note that, in the wall region, where the average liquid velocity is downward, bubbles can move upward as well as downward while the most probable velocity value takes into account axial ascending bubble velocity only. Consequently, the most probable velocity measurement significantly overestimates the actual mean bubble velocity in the vicinity of walls.

However, major errors due to lateral motion are avoided, as the inter-correlation function exhibits a very clear maximum at τ_{max} (cf. Fig. 13).

To estimate the reliability of the most probable velocity, the correlation coefficient, k, is calculated:

$$k = \frac{\sum_t (X_1(t) - \overline{X}_1)(X_2(t+\tau) - \overline{X}_2)}{\sum_t (X_1(t) - \overline{X}_1)^2 \sum_j (X_2(t+\tau) - \overline{X}_2)^2} \quad (6)$$

where $X_i(t)$ is the binarized signal from fibre i.

To obtain reliable data, it is commonly admitted [26] that this coefficient should be greater than 0.7. A smaller coefficient corresponds to poorly correlated signals X_1 and X_2. That is the case in this work: values of k lay between 0.4 and 0.8.

The plot of k versus radial position presented in Fig. 14 for two gas velocities shows that k does not depend on superficial gas velocity (in the tested range). However, the trend for k depends on liquid media: k is greater in cyclohexane than in water, in accordance with previous observations, assuming more complex flow in water. k depends on radial position too: k decreases in the near wall region, where liquid flows downwards. This point confirms the previous observations: near the wall, frequent inversion of bubble velocity leads to poor signal correlation and to poor velocity reliability.

To evaluate the relevance of bubble velocity, the space averaged superficial gas velocity calculated through the integration over a column section of $(\varepsilon_G * \tilde{v})$ has been compared to the superficial gas velocity injected in the column (Fig. 15). A convenient agreement (20%) is observed at low superficial gas velocity, when gas recirculation is weak: the

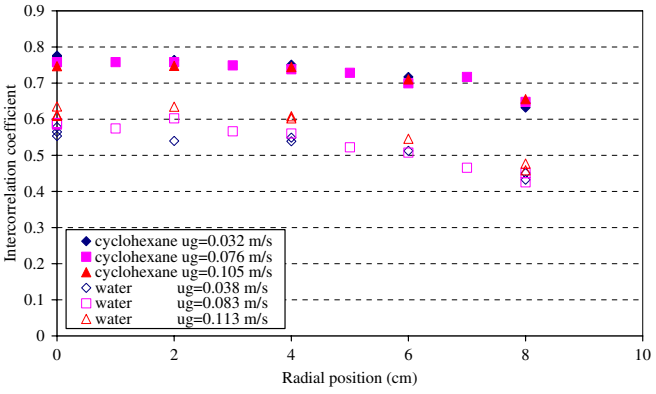

Fig. 14. Radial profiles in inter-correlation coefficient (k).

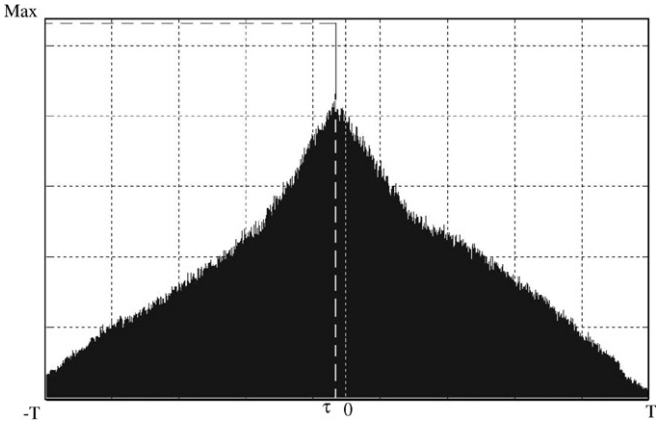

Fig. 13. Usual example of inter-correlation function.

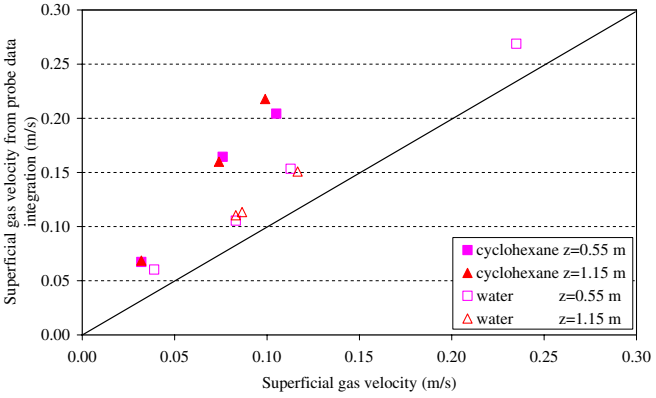

Fig. 15. Comparison of superficial gas velocity with the integration over a column section of $(\varepsilon_G * \tilde{v})$.

measured bubble velocities are reliable in these conditions. The deviation at higher gas velocities comes then mainly from downward velocities, not seen by the optic probe. The gas velocity overestimation by the optic probe is much larger in cyclohexane (up to 100%) than in water (about 20%). It could be due to the well-known bad detection by the optic probe of the very short bubbles, as such bubbles are more numerous in cyclohexane [27].

Fig. 15 also shows that, for both liquids, the axial position has no influence on the results: the flow in bubble column looks already established at 0.5 m.

To conclude, the comparison between the measured most probable velocity and the actual gas velocity shows that the optic probe provides the most probable ascendant velocity (a closer value to the mean velocity in water than in cyclohexane).

4.4. Bubble size

Individual bubble chord can in theory be determined from individual bubble velocity and residence time. It was shown that individual bubble velocity is not fully reliable. Therefore the chords distribution is not realistic (even in the little tank [9]). This approach was not worked out here. The validity of the mean bubble diameter calculation, using the most probable velocity through Eq. (5), is discussed.

Fig. 16 presents radial profiles of mean Sauter diameters in both media. These profiles are quite flat and show bigger bubbles in water, in accordance with its larger surface tension. Of course those data give orders of magnitude only, as bubbles of 4–8 mm can not be spherical, as implicitly assumed in Eq. (5).

As a conclusion, this methodology leads to the estimation of mean Sauter diameter. Although those values are not very precise, they are essential:

- They give an estimation of local interfacial area, which is an essential parameter for mass transfer and which is rarely determined in complex flows.
- They allow a comparison between different conditions.

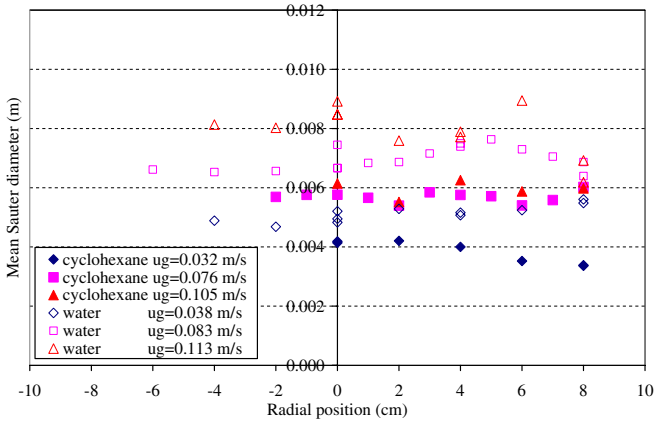

Fig. 16. Mean Sauter diameter profiles.

5. Conclusions and perspectives

In this study, a methodology for double optic probe data treatment has been established for complex flows.

Gas hold-up and bubble frequency can be easily obtained and those data are reliable. However, the estimation of bubble velocity and bubble diameter is more hazardous. A previous study, realised in a little tank with distorted tumbling bubbles [9], has already shown the difficulty to obtain distributions, particularly size ones. The methodology proposed in this study is attempted here in a more complex flow. It appears that a treatment using only mean local values is preferable and gives reliable orders of magnitude of ascending bubble velocity and bubble size. The velocity is estimated through the most probable velocity issued from the inter-correlation of both raw signals; the average bubble diameter is estimated through Eq. (5):

$$d_{SM} = \frac{3\tilde{v}\varepsilon_G}{2f_B} \tag{5}$$

Even if the obtained data are not very precise yet – some progresses are still necessary in this way – this methodology allows a better knowledge of complex flows in large bubble columns at high gas hold-up.

References

[1] C. Boyer, A.-M. Duquenne, G. Wild, Measuring techniques in gas–liquid and gas–liquid–solid reactors, Chemical Engineering Science 57 (2002) 3185–3215.

[2] M. Utiger, F. Stuber, A.M. Duquenne, H. Delmas, C. Guy, Local measurements for the study of external loop airlift hydrodynamics, Canadian Journal of Chemical Engineering 77 (1999) 375–382.

[3] A. Larue de Tournemine, Etude expérimentale de l'effet du taux de vide en écoulements diphasiques à bulles, INPT thesis, Toulouse, France, 2001.

[4] H.H. Bruun, Hot Wire Anemometry. Principles and Signal Analysis, Oxford University Press, Inc., New York, 1995.

[5] J.M. Schweitzer, J.M. Bayle, T. Gauthier, Local gas hold-up measurements in fluidized bed and slurry bubble column, Chemical Engineering Science 56 (2001) 1103–1110.

[6] J. Werther, Bubbles in gas fluidized beds, Transactions of the Institution of Chemical Engineers, Part I 52 (1974) 149–159.

[7] N.N. Clark, R. Turton, Chord length distributions related to bubble size distributions in multiphase flow, International Journal of Multiphase Flow 14 (1988) 413–424.

[8] S.T. Revankar, M. Ishii, Local interfacial measurement in bubbly flow, International Journal of Heat and Mass Transfer 35 (1992) 913–925.

[9] H. Chaumat, A.-M. Billet-Duquenne, F. Augier, C. Mathieu, H. Delmas, Application of the double optic probe technique to distorted tumbling bubbles in aqueous and organic liquid, Chemical Engineering Science 60 (2005) 6134–6146.

[10] S. Hogsett, M. Ishii, Local two-phase flow measurements using sensor techniques, Nuclear Engineering and Design 175 (1997) 15–24.

[11] D.J. Gunn, H.H. Al-Doorin, The measurement of bubble flow in fluidized beds by electrical probe, International Journal of Multiphase Flow 11 (1985) 535–551.

[12] S. Moujaes, R.S. Dougall, Experimental investigation of cocurrent two-phase flow in a vertical rectangular channel, Canadian Journal of Chemical Engineering 65 (1987) 705–715.

[13] K.H. Choi, W.K. Lee, Comparison of probe methods for measurement of bubble properties, Chemical Engineering Community 91 (1990) 35–47.

[14] C.-S. Lo, S.-J. Hwang, Local hydrodynamic properties of gas phase in an internal-loop airlift reactor, Chemical Engineering Journal 91 (2003) 3–22.
[15] A. Kamp, Ecoulements turbulents à bulles dans une conduite en micropesanteur, PhD thesis, INPT, France, 1996.
[16] S. Saberi, K. Shakourzadeh, D. Bastoul, J. Militzer, Bubble size and velocity measurement in gas–liquid systems: application of fiber optic technique to pilot plant scale, Canadian Journal of Chemical Engineering 73 (1995) 253–257.
[17] I. Kataoka, M. Ishii, A. Serizawa, Local formulation and measurements of interfacial area concentration in two-phase flow, International Journal of Multiphase Flow 12 (1986) 505–529.
[18] J.M. Burgess, A.G. Fane, C.J.D. Fell, Application of an electroresistivity probe technique to a two-dimensional fluidized bed, Transactions of the Institution of Chemical Engineers 59 (1981) 249–252.
[19] B.P. Yao, C. Zheng, H.E. Gasche, H. Hofmann, Bubble behaviour and flow structure of bubble columns, Chemical Engineering Process 29 (1991) 65–75.
[20] T. Hibiki, R. Situ, Y. Mi, M. Ishii, Local flow measurements of vertical upward bubbly flow in an annulus, International Journal of Heat and Mass Transfer 46 (2003) 1479–1496.
[21] S.L. Kiambi, A.-M. Duquenne, J.B. Dupont, C. Colin, F. Risso, H. Delmas, Analysis of bubble-probe interactions by imaging: application to local interfacial measurements, Canadian Journal of Chemical Engineering 81 (2003) 764–770.
[22] N.N. Clark, R.L.C. Flemmer, Turbulent circulation in bubble columns, AIChE Journal 33 (1987) 515–518.
[23] A. Orell, On the liquid flow reversal in bubble columns, Chemical Engineering Community 115 (1992) 149–159.
[24] M. Millies, D. Mewes, Calculation of circulation flows in bubble columns, Chemical Engineering Science 50 (1995) 2093–2106.
[25] S. Kalkach-Navarro, R.T. Lahey Jr., D.A. Drew, R. Meyder, Interfacial area density, mean radius and number density measurements in bubbly two-phase flow, Nuclear Engineering and Design 142 (1993) 341–351.
[26] J.P. Galaud, Contribution à l'étude des méthodes de mesure en écoulement diphasique, applications à l'analyse statistique des écoulements à bulles, INPG thesis, Grenoble, France, 1975.
[27] H. Chaumat, A.M. Billet-Duquenne, G. Hébrard, F. Augier, C. Mathieu, H. Delmas, Influence des propriétés physico-chimiques sur la distribution de tailles de bulles, Récents Progrès en Génie des Procédés, 92, S-10, 2005.